Ann. For. Res. 57(2): 289-298, 2014
DOI: 10.15287/afr.2014.278

ANNALS OF FOREST RESEARCH
www.afrjournal.org

Estimating aboveground biomass using Landsat TM imagery: A case study of Anatolian Crimean pine forests in Turkey

A. Günlü, İ. Ercanli, E.Z. Başkent, G. Çakır

Günlü A., Ercanli İ., Başkent E.Z., Çakır G., 2014. Estimating aboveground biomass using Landsat TM imagery: A case study of Anatolian Crimean pine forests in Turkey. Ann. For. Res. 57(2): 289-298, 2014.

Abstract. Forests play an important role in carbon circulation, and the productivity of forest ecosystems can be evaluated by evaluating its biomass. Evaluation of biomass aids the determination and understanding of changes in forest ecosystems. Because of the limitations of ground measurements of biomass, in recent times, satellite images have been broadly applied to estimate aboveground biomass (AGB). The objective of this study is to examine the relationships between AGB and individual band reflectance values and ten Vegetation Indices (VIs) obtained from a Landsat TM satellite image for a Anatolian pine forests in northwestern Turkey. Multiple regression analysis is utilized to predict the AGB. The AGB model using TM 1 and TM 2 had an adjusted R^2 of 0.465. Another AGB model using Enhanced Vegetation Index (EVI) and Normalized Difference 57 (ND57) had an adjusted R2 of 0.606. Our results reveal that VIs present better estimation of AGB in Anatolian pine forests as compared to individual band reflectance values.
Keywords Aboveground biomass, Landsat TM satellite data, modelling.

Authors. Alkan Günlü (alkangunlu@karatekin.edu.tr), İlker Ercanli - Çankırı Karatekin University, Faculty of Forestry, 18200, Çankırı, Turkey; Emin Zeki Başkent - Karadeniz Technical University, Faculty of Forestry, 61080, Trabzon, Turkey; G. Çakır - Gümüşhane University, Graduate School of Natural and Applied Sciences, Department of Forestry and Environmental Science, 29000, Gümüşhane, Turkey.
Manuscript received August 19, 2013; revised October 29, 2014; accepted November 20, 2014; online first November 27, 2014.

Introduction

Forests play a significant role in maintaining global climate stability and carbon circulation. Forest ecosystem productivity can be evaluated by evaluating its biomass. Biomass estimation is very important for evaluating forest ecosystem productivity and controlling carbon budgets (Zianis & Mencuccini, 2004, Hall et al., 2006). Accurate prediction of biomass is necessary to better understand the carbon cycles in forest ecosystems, which act as a major pool of carbon (Houghton 2005). Various techniques, such as ground measurements (Schroeder et al. 1997, Houghton et al. 2001) and satellite imagery (Foody et al. 2003, Lu 2005), have been applied to estimate the amount of biomass.

Ground measurements have been used to accurately predict the aboveground biomass (AGB) by using the allometric relationship between tree height and diameter of trees at breast height. However, for large forest areas, this technique is often very time and labor consuming (Lu 2006). Recently, satellite images have been broadly applied to monitor and predict the AGB over larger areas (Goetz et al. 2009, Houghton et al. 2009, Gallaun et al. 2010). In particular, Landsat satellite imagery has been utilized as a main resource in many applications to predict the AGB of small and/ or large areas. However, different optical satellite images such as Aster (Muukkonen & Heiskanen 2005), Ikonos (Thenkabail et al. 2004), MODIS (Baccini et al. 2004), NOAA AVHRR (Dong et al. 2003), and WorldView-2 (Eckert 2012) have been used for estimating biomass. Generally, the AGB can be estimated from satellite images by using various techniques such as multiple regression analysis and k-nearest-neighbor classification (Zheng et al. 2004, Labrecque et al. 2006, Ji et al. 2012).

However, the ability to estimate forest biomass from passive satellite images is limited because the spectral responses in passive satellite images are primarily connected to the interface between sun radiance and stand crown closures. Therefore, in general, the relationship between AGB and Vis or spectral reflectance values is low (Lu 2006, Sarker & Nichol 2011). Recent studies have demonstrated that the use of SAR satellite images such as radar or lidar can result in more successful biomass estimates as compared to those from optical satellite images (Lu 2006, Wang & Qi 2008, Goetz et al. 2009). Many studies have indicated the potential of using active satellite images (radar) for predicting AGB (Kuplich et al. 2000, Wang & Qi 2008), and active remote sensing data (airborne laser) has been utilized to estimate aboveground (Naesset 2011) and tree biomass (Nyström et al. 2011). Lidar and radar satellite images have also been used to estimate the biomass in different forest structures (Saatchi et al. 2011, Zhao et al. 2012, Zalkos et al. 2013). Previous studies have shown that long-wavelength data, such as that from radar or lidar, is useful for predicting the AGB of forests with complex structures (Lim et al. 2003, Zimble et al. 2003). However, active remote sensing images require extra processing such as pre-processing, subtraction of noise, and image processing. Additionally, active remote sensing data is more expensive than other satellite images, such as Ikonos and QuickBird. Therefore, in general, radar or lidar data has not been sufficiently useful for predicting the AGB in large areas. Medium resolution satellite images offer the potential for predicting AGB at the regional level. However, problems such as mixed pixels and image saturation in medium resolution satellite images are found when estimating AGB from them. The spectral reflection of Landsat TM satellite images is more appropriate for AGB estimation in a simple forest structure.

This study focuses mainly on evaluating the relationship between band reflectance values and VIs from a Landsat TM satellite image and the AGB obtained from ground measurements by using multiple regression analysis for Anatolian pine forests in northwestern Turkey.

Material and methods

Study area

The study area is the Buyukduz planning unit located in Karabuk city in northwestern Turkey (Fig. 1). The elevation ranges from 800 to 1736 m above sea level and is 1270 m on average. The study area has an average slope of 45%.

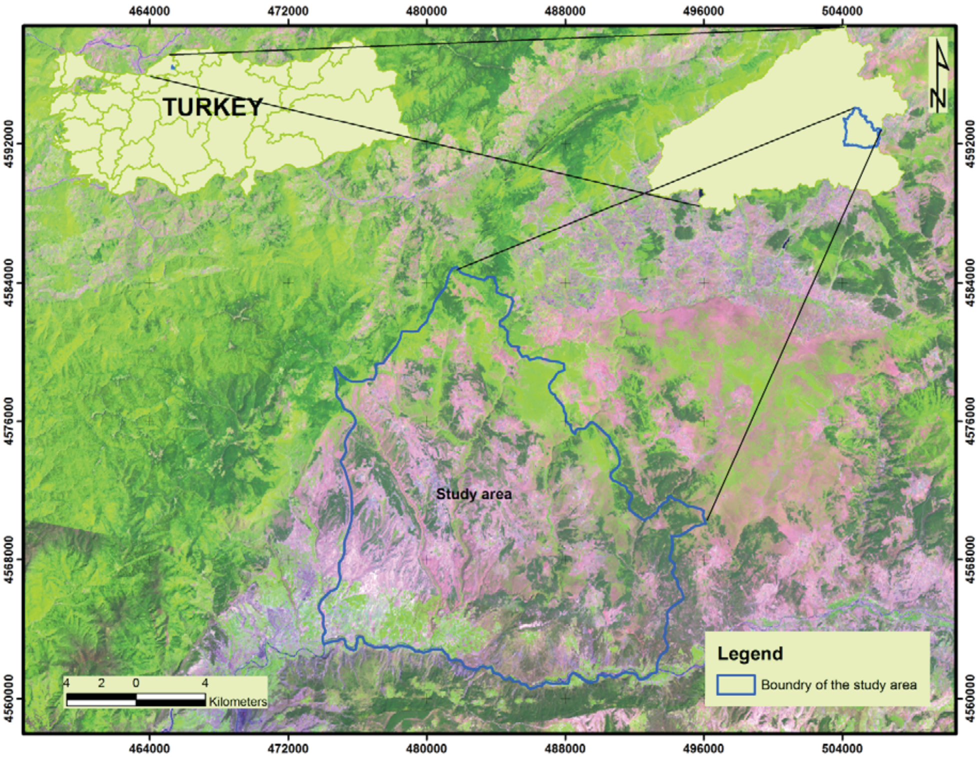

Figure 1 Location of the study area

Mean annual temperature and precipitation are 12.0°C and 650 mm, respectively. 393.3 ha (2.3%) of the study area is covered with fir [*Abies nordmanniana* (Stev.) Spach. subsp. *bornmuelleriana* (Mattf.)], 490.4 ha (2.9%) with Scotch pine (*Pinus sylvestris* L.), 10246.0 ha (60.9%) with Anatolian Crimean pine [*Pinus nigra* Arnold. subsp. *pallasiana* (Lamb.) Holmboe], 274.4 ha (1.6%) with beech (*Fagus orientalis* Lipsky), 3416.5 ha (20.5%) with Çoruh oak [*Quercus petraea* subsp. *iberica* (Steven ex Bieb.) Krassilin], and 1094.2 ha (11.8%) with *Pinus brutia* Ten.

Ground measurements and aboveground biomass estimation

Ground measurements were conducted in the summer of 2010. In total, 130 sample plots of pure Crimean pine forest areas were developed and investigated. The size of the circular sample plots ranged from 400 to 800 m^2, depending on stand crown closure. A Global Positioning Systems (GPS) receiver was placed at the center of every sample plot. UTM coordinates of every sample plot were also recorded by GPS. In these sample plots, the diameter of every tree at breast height (dbh) was measured to the nearest 0.1 cm using calipers with dbh > 7.9 cm. The AGB of each tree was calculated using the following equation (Equation 1–3) developed by Çakıl (2008) for Anatolian pine trees.

Tree stem:

$$Y = 0.10335\, d^2_{1.30} + 9.773876\, d_{1.30} - 103.221 \quad (1)$$

Branch:

$$Y = 15.72827\, Ln(d_{1.30}) - 35.8478 \quad (2)$$

Needle:

$$Y= 0.709426 + 0.002182\, d^2_{1.30} \quad (3)$$

where $d_{1.30}$ - diameter at breast height.

When calculating the AGB in the sample plots, the biomass amount of individual trees was summarized and converted to a per hectare unit based on the size of the sample plots.

Remote sensing data and processing

Landsat TM satellite data acquired on September 3, 2010 was used in this study. The first six bands, TM 1 (0.45–0.52μm), TM 2 (0.52–0.60 μm), TM 3 (0.63–0.69 μm), TM 4 (0.76–0.90 μm), TM5 (1.55–1.75 μm), and TM 7 (2.08–2.35 μm), with 30 m spatial resolution were used. The Landsat TM satellite data was georeferenced to UTM WGS 84 Zone 36. Using 20 control points taken from 1/25.000 scale topographic maps using the nearest-neighbor method, a root square mean error of 0.5 pixels was obtained, which translates to a ±15 m ground accuracy. The locations of the sample plots and test points were determined by GPS. However, the GPS points have positional errors, which normally average to ±4m. Therefore, it is nearly impossible to accurately locate every sample plot and test point on the center of the 30 m grid of Landsat TM pixels. To solve this location problem, many researchers used a moving window, such as a 3 x 3 pixel (Makela and Pekkarinen 2004, Labrecque et al. 2006) one. We used a moving window to average the spectral reflectance values in the surrounding pixels. In each sample plot, the spectral reflectance values of nine pixels were averaged by using a 3×3 window. Then, the VIs were calculated according to the reflectance values of each sample plot. In this study, ten VIs were calculated from six individual bands (except Band 6) as independent variables. The VI formulas used in this study are listed in Table 1. The Erdas Imagine 9.1™ software was utilized for data processing.

Statistical analyses

Stepwise multiple regression analysis was used to investigate and model the relationship between the spectral reflectance values of TM 1–5, TM 7, and ten VIs, from the Landsat TM satellite data, and the AGB values. The stepwise multiple regression models were improved by using Landsat TM satellite data, band spectral reflectance values and VIs, and their combination as independent variables to improve the AGB estimation. The dependent variable was the AGB values. The regression models were improved to forecast the AGB as a function of a suite of Landsat TM satellite data variables gathered for the case forest

Table 1 Definition of vegetation indices used in the study area

Vegetation indices	Formula	Reference
Normalize Difference Vegetation Index (NDVI)	*(TM4-TM3)/(TM4+TM3)*	Rouse et al. (1973)
Simple Ratio (SR)	*(TM4)/(TM3)*	Jordan (1969)
Difference Vegetation Index (DVI)	*(TM4)-(TM3)*	Clevers (1988)
Soil Adjusted Vegetation Index (SAVI)	*(TM4-TM3)*(1+L)/(TM4+ TM 3+L)*	Huete (1988)
Normalized Difference (ND)53	*(TM 5)-(TM 3)/(TM 5)+(TM 3)*	Lu et al. (2004)
Normalized Difference (ND)54	*(TM 5)-(TM 4)/(TM 5)+(TM 4)*	Lu et al. (2004)
Normalized Difference (ND)57	*(TM 5)-(TM 7)/(TM 5)+(TM 7)*	Lu et al. (2004)
Normalized Difference (ND)32	*(TM 3)-(TM 2)/(TM 3)+(TM 2)*	Lu et al. (2004)
Normalized Difference (ND)73	*(TM 7)-(TM 3)/(TM 7)+(TM 3)*	Sivanpillai et al. (2006
Enhanced Vegatation Index (EVI)	*(TM 4- TM 3))/((TM 4+(C1·TM 3)-(C2·TM2)·(1+L))*	Huete et al. (1999)

site. The AGB value was modeled with Landsat TM satellite data using stepwise multiple linear regression. In the stepwise variable selection method, the process starts out just as in forward selection. However, at each step, the variable that is already in the model is first evaluated for removal. The variable whose removal results in the smallest R^2 is removed first from the variables that are eligible for removal. The multiple stepwise regression analysis was carried out by SPSS (SPSS Institute Inc 2007). This analysis was utilized to determine the best predictive variables that were significant ($p < 0.05$), with the highest value of the determination of coefficient (R^2_{adj}). In this study, the subsequent linear relationship was assumed (Equation-4):

$$AGB = \beta_0 + \beta_1 \cdot X_1 + \beta_2 \cdot X_2 + ... + \beta_n \cdot X_n + \varepsilon \quad (4)$$

where AGB is the aboveground biomass, X_1 … X_n are variable vectors corresponding to Landsat TM satellite data values, such as the spectral reflectance values, TM 1–5 and TM 7, and the ten VIs, $\beta_1 ... \beta_n$ characterize the model coefficients and ε is the additive bias (Corona et al. 1998).

To compare the predictive power of the spectral reflectance values, for e.g., for TM 1–5, TM 7, and VIs, separate regression analysis was performed using relevant Landsat TM satellite data. Therefore, two regression models were developed (the AGB and Landsat TM spectral reflectance values and the AGB and VIs) for predicting the AGB; one by using the band spectral reflectance values and the other by using the VIs. In each model sub-group, the related AGB was estimated by using the spectral reflectance values in TM 1–5 and TM 7, and VIs. The regression models were evaluated based on the accuracy statistics. The accuracy statistics covered the absolute and relative biases and the root mean square error (*RMSE* and *RMSE*%). These statistics were calculated for the models as the following (Equation 5–8):

$$bias = \frac{\sum (y_i - \hat{y}_i)}{n} \quad (5)$$

$$bias\% = 100 \frac{\sum (y_i - \hat{y}_i) / n}{\sum \hat{y}_i / n} \quad (6)$$

$$RMSE = \sqrt{\frac{\sum (y_i - \hat{y}_i)^2}{n-1}} \quad (7)$$

$$RMSE\% = 100 \frac{\sqrt{\sum (y_i - \hat{y}_i)^2 / (n-1)}}{\sum \hat{y}_i / n} \quad (8)$$

where n is the number of observations, and y_i and $\hat{y}_i$ are observed and predicted values of the aboveground biomass from developed models. To further assess the superiority of the model fit, we used the magnitude and distribution of predicted values versus observed ones for the AGB using Landsat TM data. We examined any obvious dependencies or patterns representing systematic divergences and a breakdown of assumptions of multiple least-square regressions. The presence of multicollinearity was defined by values of the variance inflation factors (VIF), with values greater than five taken to indicate the presence of multicollinearity (Myers 1986).

Results

The selected best regression models provided accuracy statistics like coefficients of determination (R^2_{adj}), standard error of the model ($S_{y.x}$), *bias, bias*%, *RMSE, RMSE*% and Durbin-Watson (*DW*) values. The AGB prediction models were developed based on a combination of ground measurements and the Landsat TM satellite image. Table 2 and Table 3 summarize the best regression models for the AGB based on individual band reflectance values and VIs obtained from the Landsat TM satellite image. In these selected regression models for the AGB, the F statistics and coefficients were significant at a probability level of 95%.

The regression model that used TM 1 and TM 2 as independent variables had an R^2_{adj} of 0.465 and *RMSE* of 9.1836 t ha^{-1} (Table 2). Furthermore, the other model, which used the EVI and ND57 as independent variables, had an R^2 of 0.606 and *RMSE* of 8.5054 t ha^{-1} (Table 3). The results obtained from the models demonstrate that VIs can better predict AGB when compared with other combinations of Landsat TM individual band spectral reflectance values. In addition, to test for multicollinearity, the variance inflation factor (VIF) values were estimated for each independent variable in the models. The VIF values ranged from 2.013 to 3.024 in the AGB model based on the spectral reflectance values. The VIF values ranged from 1.003 to 1.004 in the model based on VIs. Since all VIF values were lower than five for the sub-group models, there appears to be no problem of multicollinearity for the independent variables of these models (Table 2-3).

Discussion

In this study, regression models were employed for predicting the relationships between AGB and the reflectance values and VIs obtained from a Landsat TM satellite image. The results indicate that a linear combination of the Landsat TM 1 and TM 2 bands is a better predictor of AGB (R^2 = 0.465, *RMSE* = 9.1836 t/ha^{-1}) than the other TM bands. TM 1 has a negative relationship with AGB, but TM 2 has a positive relationship (Table 2). The negative relationship may be due to the following reasons; (a) increased crown closure shadowing in larger forest areas and/or (b) decreased understory reflectance values owing to raised intensity with AGB increases (Spanner et al. 1990). The positive relation is explained by the increased reflectance values based on the AGB increases. In addition, the model that included EVI and ND57 as predictor variables better predicted the AGB (R^2_{adj} = 0.606, *RMSE* = 8.5054 t/ha^{-1}) than that using other VIs. Our results demonstrate that using VIs obtained from Landsat

Table 2 Parameters of the 'Best fit' regression models of stand biomass based the spectral reflectance values, TM 1-5 and TM 7

Independent variables	Coefficients of independent variables	S. E. of variables	*t*-statistics	*p*-value	*VIF*
Constant	7.405	0,300277	24.659	0.000	
TM 1	-0.10095	0,012948	-7,79690	0.000	3.024
TM 2	0.089591	0,016944	5,287218	0.000	2.013

Note. Related measures: R^2_a = 0.465, *Sy.x* = 0.2239, *D.W.* = 2.016, *Bias* = 1.9906, *Bias*% = 2.3778, *RMSE* = 9.1836, *RMSE*% = 10.9697

Table 3 Parameters of the 'Best fit' Regression models of stand biomass based the vegetation indices

Independent variables	Coefficients of independent variables	S. E. of variables	t-statistics	p-value	VIF
Constant	2,40192	0,14822	16,20435	0.000	
ND57	4,76912	0,35412	13,46752	0.000	1.003
EVI	0,00403	0,00079	5,059291	0.000	1.004

Note. Related measures: R^2_a = 0.606, *Sy.x* = 0.20687, *D.W.* = 1.982, *Bias* = 1.7055, *Bias*% = 2.0433, *RMSE* = 8.5054, *RMSE*% = 10.1896

TM is more successful for AGB prediction than using individual Landsat TM band reflectance values since VIs can maximize the sensitivity for recording the green vegetation situation. Furthermore, VIs can minimize the impacts of topography, sun angles, canopy geometry, soil background, and atmospheric changeability, and therefore their relationship with the AGB can be more straightforward (Lu et al. 2005). VIs have also been suggested to be good indicators for estimating biomass and LAI (Verrelest et al. 2008). Our results also agree with some previous studies that indicated a correlation between AGB and VIs (Heiskanen 2006, Maynard et al. 2007). However, some studies have demonstrated little correlation between AGB and VIs (Foody et al. 2003, Schlerf et al. 2005).

Dahlberg (2001) stated that the TM 3 band is the best predictor of biomass in the birch forests in Sweden. However, no relationship was observed between TM 3 and AGB in our study. Using a multiple regression model, Lu et al. (2002) found that the AGB was estimated well when individual band reflectance values and VIs obtained from Landsat TM were used (R^2 = 0.88). Zheng et al. (2004) estimated the AGB by splitting the sample plots into hardwoods and softwoods. Hardwood AGB was roughly related with stand age and TM 4 (R^2 = 0.95), while softwood AGB was strongly related with NDVIc (R^2 = 0.84). Lu (2005), when estimating the AGB using Landsat satellite images for five different areas, showed that the AGB was highly correlated with the TM 5 (R^2 = 0.683), TM 4 (R^2 = 0.701), and TM 4 (R^2 = 0.746), but had a low linear relationships with the ND54 (R^2 = 0.404) and TM 5 (R^2=0.158). Heiskanen (2006) modeled the AGB using Aster satellite data in birch forest areas and the AGB models were found be appropriate with an R^2 = 0.81 with SR, R^2 = 0.79 with SAVI2, R^2 = 0.78 with RSR, and R^2 = 0.76 with log (band 2). Zheng et al. (2007) modeled the AGB using Landsat ETM+ data and ground data for four different forest stands (Chinese fir, conifer, broadleaf, and mixed forest). The AGB models using VIs were developed using LAI-NDVI, LAI-Age, Age, and LAI-SR as independent variables and gave an R^2 of 0.930, 0.937, 0.792, and 0.931, respectively. Maynard et al. (2007) modeled the AGB using VIs and spectral reflectance values generated from Landsat 7 ETM+ satellite data and the R^2 was 0.41 for NDVI, 0.44 for SAVI, 0.51 for GVI and WI, and 0.53 for ETM 4 and ETM 7. Gaspari et al. (2010) studied the relationship between the AGB in subtropical dry forests of Argentina using individual band reflectance values and VIs obtained from Landsat 7 ETM+ satellite images. Their models predicted the AGB with an R^2 of 0.581 for ETM 7, 0.560 for ETM 3, 0.436 for ETM 5, and 0.636 for NDVI. Another study by Das and Singh (2012) on the estimation of AGB using VIs obtained from Landsat TM satellite data had an R^2 of 0.75 for NDVI, 0.76 for RDVI, 0.70 for MSR, 0.78 for RVI, 0.67 for MSAVI, and 0.75 for OSAVI. In general, most of the studies described above indicate significant relationships between the AGB and individual band reflectance values. However, in contrast to most of the above studies, a good relationship between AGB and VIs was found in this study. In addition, forest biomass predicted with VIs based on the Landsat satellite image has been shown to not be suitable for complex forest areas (Zheng et al. 2004). In order to achieve better results of the relationship between AGB and VIs or reflectance values, it would be better to use alternative high-resolution satellite images such as QuickBird, Ikonos, and WorldView-2. However, these satellite images are not appropriate for large areas owing to the expenditure in obtaining the satellite data, and the enormous amount of time required for processing. Active remote sensing data such as radar or lidar may well be appropriate for predicting forest biomass in simple forest structures (Lu 2006). However, for large areas, especially for Turkish forest areas, active satellite imagery is more expensive to collect than other satellite data. Therefore, a mix of multi-scale remote sensing data (coarse, medium, and fine resolution) can be used to more accurately estimate the AGB at different scales.

Conclusions

Using a Landsat TM satellite image, regression models were developed using independent variables (TM 1-5 and TM 7 and ten VIs) to estimate the AGB in Anatolian Crimean pine forests in northwestern Turkey. Our results shows that VIs can better estimate the AGB as compared to individual band spectral reflectance values. The most suitable band reflectance values and VIs will depend upon factors such as study aims, geographic position and structure of forest areas, scaling issues, mixed pixel condition, and timing of satellite data. Therefore, more detailed studies need to be performed to develop an appropriate method that can be applied to different forest ecosystems. Our study shows that regression models using VIs obtained from Landsat TM satellite data can be beneficial for modeling the AGB in conifer forest areas that have similar forest ecosystems as our study area.

Acknowledgements

The authors would like to thank to for support to the Head of Forest Management and Planning Department, General Directorate of Forestry, Republic of Turkey.

References

Baccini A., Friedl M.A., Woodcock C.E., Warbington R., 2004. Forest biomass estimation over regional scales using multisource data. Geophysical Research Letters 31: L10501, doi: 10.1029.

Boegh E., Broge H.S.N., Hasager C.B., Jensen N.O., Schelde K., Thomsen A., 2002. Airborne multispectral data for quantifying leaf area index, nitrogen concentration, and photosynthetic efficiency in agriculture. Remote Sensing of Environment 81: 179−193. DOI: 10.1016/S0034-4257(01)00342-X.

Brown S., 2002. Measuring carbon in forests: current status and future challenges. Environmental Pollution 116(3): 363-372. DOI: 10.1016/S0269-7491(01)00212-3.

Çakıl E., 2008. Constructing biomass tables of Crimean pıne in Zonguldak Forest Administration. Master Thesis, Zonguldak Karaelimas University, P. 167, Institute of Science.

Clevers J.G.P.W., 1988. The derivation of a simplified reflectance model for the estimation of leaf area index. Remote Sensing of Environment 25: 53–70. DOI: 10.1016/0034-4257(88)90041-7.

Corona P., Scotti R., Tarchiani N., 1998. Relationship between environmental factors and site index in Douglas-fir plantations in central Italy. Forest Ecology and Management 101: 195-207. DOI: 10.1016/S0378-1127(98)00281-3.

Das S., Singh T.P., 2012. Correlation analysis between biomass and spectral vegetation indices of forest ecosystem. International Journal of Engineering Research and Technology Vol. 1 Issue 5.

Dong J., Kaufmann R.K., Myneni R.B., Tucker C.J., Kauppi P.E., Liski J., Buermann W., Alexeyev V., Hughes M.K., 2003. Remote sensing estimates of boreal and temperate forest woody biomass: carbon pools, sources, and sinks. Remote Sensing of Environment 84: 393–410. DOI: 10.1016/S0034-4257(02)00130-X.

Eckert S., 2012. Improved Forest Biomass and Carbon Estimations Using Texture Measures from WorldView-2 Satellite Data. Remote Sensing 4(4): 810-829. DOI: 10.3390/rs4040810.

Fazakas Z., Nilsson M., Olsson H., 1999. Regional forest biomass and wood volume estimation using satellite data and ancillary data. Agricultural and Forest Meteorology 98–99: 417–425. DOI: 10.1016/S0168-1923(99)00112-4.

Fontes L., Tome M., Thompson F., Yeomans A., Luis J.S., Savill P., 2003. Modelling the Douglas-fir (Pesudotsuga menziesii (Mirb.) Franco) site index from site factors in Portugal. Forestry 76: 491-507. DOI: 10.1093/forestry/76.5.491.

Foody G.M., Cutler M.E., Mcmorrow J., Pelz D., Tangki H., Boyd D.S., Douglas I., 2001. Mapping the biomass of Bornean tropical rain forest from remotely sensed data. Global Ecology and Biogeography 10:379–387. DOI: 10.1046/j.1466-822X.2001.00248.x.

Foody G.M., Boyd D.S., Cutler M.E.J., 2003. Predictive relations of tropical forest biomass from Landsat TM data and their transferability between regions. Remote Sensing of Environment 85: 463–474. DOI: 10.1016/S0034-4257(03)00039-7.

Goetz S.J., Baccini A., Laporte N.T., Johns T., Walker W., Kellndorfer J., Houghton R.A,. Sun M. 2009. Mapping and monitoring carbon stocks with satellite observa-

tions: a comparison of methods. Carbon Balance and Management 4, 2. DOI: 10.1186/1750-0680-1184-1182.
Hall R.J., Skakun R.S., Arsenault E.J., 2006. Modeling forest stand structure attributes using Landsat ETM+ data: Application to mapping of aboveground biomass and stand volume. Forest Ecology and Management 225: 378–390. DOI: 10.1016/j.foreco.2006.01.014.
Hame T., Salli A., Andersson K., Lohi A., 1997. A new methodology for the estimation of biomass of conifer-dominated boreal forest using NOAA AVHRR data. International Journal of Remote Sensing 18: 3211–3243. DOI: 10.1080/014311697217053.
Heiskanen J., 2006. Estimating aboveground tree biomass and leaf area index in a mountain birch forest using ASTER satellite data. International Journal of Remote Sensing 27: 1135–1158. DOI: 10.1080/01431160500353858.
Houghton R.A., Lawrence K.T., Hackler J.L., Brown S., 2001. The spatial distribution of forest biomass in the Brazilian Amazon: a comparison of estimates. Global Change Biology 7: 731–746. DOI: 10.1046/j.1365-2486.2001.00426.x.
Houghton R.A., 2005. Aboveground forest biomass and the global carbon balance. Global Change Biology 11: 945–958. DOI: 10.1111/j.1365-2486.2005.00955.x.
Houghton, R. A., Hall, F., & Goetz, S. J. (2009). Importance of biomass in the global carbon cycle. Journal of Geophysical Research, 114, G00E03. DOI: 10.1029/2009JG000935. DOI: 10.1029/2009JG000935.
Huete A.R., 1988. A soil adjusted vegetation index (SAVI). Remote Sensing of Environment 25: 295–309. DOI: 10.1016/0034-4257(88)90106-X.
Huete A., Justice J., Leeuwen W., 1999. MODIS vegetation index (MOD 13) algorithm theoretical basis document version 3. Available online at: http://modis.gsfc.nasa.gov/data/atbd/atbd_mod13.pdf (accessed 1 February 2006).
Hussin Y.A., Reich R.M., Hoffer R.M., 1991. Estimating slash pine biomass using radar backscatter. IEEE Transactions on Geoscience and Remote Sensing 29: 427–431. DOI: 10.1109/36.79433.
Jordan C.F., 1969. Derivation of leaf area index from quality of light on the forest floor. Ecology 50: 663–666. DOI: 10.2307/1936256.
Kuplich T.M., Salvatori, V., Curran P.J., 2000. JERS-1/SAR backscatter and its relationship with biomass of regenerating forests. International Journal of Remote Sensing 21: 2513–2518. DOI: 10.1080/ 01431160050030600
Ji L., Wylieb B.K., Nossovc D.R., Petersona B., Waldropd M.P., McFarlandd J.W., Roverb J., Hollingsworth T.N., 2012. Estimating aboveground biomass in interior Alaska with Landsat data and field measurements. International Journal of Applied Earth Observation and Geoinformation 18:451-461. DOI: 10.1016/j.jag.2012.03.019.
Labrecque S., Fournier R.A., Luther J.E., Piercey, D., 2006. A comparison of four methods to map biomass from Landsat-TM and inventory data in western Newfoundland. Forest Ecology and Management 226: 129-144. DOI: 10.1016/j.foreco.2006.01.030.
Leblon B., Granberg H., Ansseau C., Royer A., 1993. A semi-empirical model to estimate the biomass production of forest canopies from spectral variables, part 1: relationship between spectral variables and light interception efficiency. Remote Sensing Reviews 7: 109–125. DOI: 10.1080/02757259309532170.
Lefsky M.A., Cohen W.B., Spies T.A., 2001. An evaluation of alternate remote sensing products for forest inventory, monitoring, and mapping of Douglas fir forests in western Oregon. Canadian Journal of Forest Research 31: 78–87. DOI: 10.1139/x00-142.
Lefsky M.A., Harding D., Cohen W.B., Parker G.G., Shugart H.H., 1999. Surface lidar remote sensing of basal area and biomass in deciduous forest of eastern Maryland, USA. Remote Sensing of the Environment 67: 83–98. DOI: 10.1016/S0034-4257(98)00071-6.
Lefsky M.A., Cohen W.B., Parker G.G., Harding D.J., 2002. Lidar remote sensing for ecosystem studies. BioScience 52: 19–30. DOI: 10.1641/0006-3568(2002)052[0019:LRSFES]2.0.CO;2.
Lim K., Treitz P., Wulder M., St-Onge B, Flood M., 2003. Lidar remote sensing of forest structure. Progress in Physical Geography 27: 88–106. DOI: 10.1191/0309133303pp360ra.
Lu D., 2005. Aboveground biomass estimation using Landsat TM data in the Brazilian Amazon Basin. International Journal of Remote Sensing 26: 2509–2525. DOI: 10.1080/01431160500142145.
Lu D., 2006. The potential and challenge of remote sensing-based biomass estimation. International Journal of Remote Sensing 27(7): 1297–1328. DOI: 10.1080/01431160500486732.
Makela H., Pekkarinen A., 2004. Estimation of forest stands volumes by Landsat TM imagery and stand-level field-inventory data. Forest Ecology and Management 196: 245–255. DOI: 10.1016/ j.foreco.2004.02.049.
Maynard C.L., Lawrence R.L., Nielsen G.A., Decker G., 2007. Modeling vegetation amount using bandwise regression and ecological site descriptions as an alternative to vegetation indices. GIScience and Remote Sensing 44(1): 68-81. DOI: 10.2747/1548-1603.44.1.68.
Means J.E., Acker S.A., Harding D.J., Blair J.B., Lefsky M.A., Cohen W.B., Harmon M.E., Mckee W.A., 1999. Use of large-footprint scanning airborne lidar to estimate forest stand characteristics in the western Cascades of Oregon. Remote Sensing of Environment 67: 298–308. DOI: 10.1016/S0034-4257(98)00091-1.
Muukkonen P., Heiskanen J., 2005. Estimating biomass for boreal forests using ASTER satellite data Combined with standwise forest inventory data.

Remote Sensing of Environment 99: 434–447 DOI: 10.1016/j.rse.2005.09.011.

Myers R.H., 1986. Classical and modern regression with applications. Boston, Duxbury Press., 359 p.

Næsset E.. 2011. Estimating above-ground biomass in young forests with airborne laser scanning. International Journal of Remote Sensing 32(2): 473–501. DOI: 10.1080/01431160903474970

Nelson R., Oderwald R., Gregoire T.G., 1997. Separating the ground and airborne laser sampling phases to estimate tropical forest basal area, volume, and biomass. Remote Sensing of Environment 60: 311–326. DOI: 10.1016/S0034-4257(96)00213-1.

Nelson R.F., Kimes D.S., Salas W.A., Routhier M., 2000. Secondary forest age and tropical forest biomass estimation using Thematic Mapper imagery. Bioscience 50:419–431. DOI: 10.1641/0006-3568(2000)050[0419:SFAATF]2.0.CO;2.

Nyström M., Holmgren J., Olsson, H. 2012. Prediction of tree biomass in the forest– tundra ecotone using airborne laser scanning. Remote Sensing of Environment 123: 271–279. DOI: 10.1016/ j.rse.2012.03.008.

Phua M., Saito H., 2003. Estimation of biomass of a mountainous tropical forest using Landsat TM data. Canadian Journal of Remote Sensing 29: 429–440. DOI: 10.5589/m03-005.

Rouse J.W., Haas R.H., Schell J.A., Deering D.W., Harlan J.C., 1973. Monitoring the vernal advancement and retrogradation (green wave effect) of natural vegetation, NASA/GSFC Type III Final Report, Greenbelt, MD.

Roy P.S., Ravan S.A., 1996. Biomass estimation using satellite remote sensing data-an investigation on possible approaches for natural forest. Journal of Bioscience 21: 535–561. DOI: 10.1007/BF02703218.

Saatchi S., Marlier M., Chazdon R.L., Clark D.B., Russell A.E., 2011. Impact of spatial variability of tropical forest structure on radar estimation of aboveground biomass. Remote Sensing of Environment 115(11): 2836–2849. DOI: 10.1016/j.rse.2010.07.015.

Sarker L.R., Nichol E.J., 2011. Improved forest biomass estimates using ALOS AVNIR-2 texture indices. Remote Sensing of Environment 115: 968-977. DOI: 10.1016/j.rse.2010.11.010.

Schlerf M., Alzberger C., Hill J., 2005. Remote sensing of forest biophysical variables using HyMap imaging spectrometer data. Remote Sensing of Environment 95: 177-194. DOI: 10.1016/j.rse.2004.12.016.

Schroeder P., Brown S., Mo J., Birdsey R., Cieszewski, C., 1997. Biomass estimation for temperate broadleaf forests of the US using inventory data. Forest Science 43: 424–434.

Sivanpillai R., Smith C.T., Srinivasan R., Messina M.G., Wu X.B., 2006. Estimation of managed loblolly pine stand age and density with Landsat ETM+ data. Forest Ecology and Management 223: 247–254. DOI: 10.1016/j.foreco.2005.11.013.

Spanner M.A., Pierce L.L., Peterson D.L., Running S.W., 1990. Remote sensing of temperate coniferous forest leaf area index. The influence of canopy closure, understory vegetation and background reflectance. International Journal of Remote Sensing 11: 95–111. DOI: 10.1080/01431169008955002.

SPSS., 2007. Institute Inc. SPSS Base 15.0 User's Guide.

Steininger M.K., 2000. Satellite estimation of tropical secondary forest aboveground biomass data from Brazil and Bolivia. International Journal of Remote Sensing 21:1139–1157. DOI: 10.1080/ 014311600210119.

Thenkabail P.S., Stucky N., Griscom B.W., Ashton M.S., Diels J., Van Der Meer B., Enclona E., 2004. Biomass estimations and carbon stock calculations in the oil palm plantations of African derived savannas using IKONOS data. International Journal of Remote Sensing 25: 5447–5472. DOI: 10.1080/01431160412331291279.

Tucker C., 1979. Red and photographic infrared linear combination for monitoring vegetation. Remote Sensing of Environment 8: 127-150. DOI: 10.1016/0034-4257(79)90013-0.

Wang C., Qi J., 2008. Biophysical estimation in tropical forest using JERS-1 SAR and VNIR imagery II: Aboveground woody biomass. International Journal of Remote Sensing 29: 6827-6849. DOI: 10.1080/01431160802270123.

Zalkos S.G., Goetz S.J., Dubayah R., 2013. A meta-analysis of terrestrial aboveground biomass estimation using lidar remote sensing. Remote Sensing of Environment 128: 289-298. DOI: 10.1016/j.rse.2012.10.017.

Zhao F., Guo Q., Kelly M., 2012. Allometric equation choice impacts lidar-based forest biomass estimates: A case study from the Sierra National Forest, CA. Agricultural and Forest Meteorology 165:64-72. DOI: 10.1016/j.agrformet.2012.05.019.

Zheng D., Rademacher J., Chen J., Crow T., Bresee M., Le Moine J., Ryu S., 2004. Estimating aboveground biomass using Landsat 7 ETM+ data across a Biomass estimation managed landscape in northern Wisconsin, USA. Remote Sensing of Environment 93: 402–411. DOI: 10.1016/j.rse.2004.08.008.

Zianis D., Mencuccini, M., 2004. On simplifying allometric analyses of forest biomass. Forest Ecology and Management 187(2-3): 311-332. DOI: 10.1016/j.foreco.2003.07.007.

Zimble D.A., Evans D.L., Carson G.C., Parker R.C., Grado S.C., Gerard P.D., 2003. Characterizing vertical forest structure using small-footprint airborne lidar. Remote Sensing of Environment 87: 171–182. DOI: 10.1016/S0034-4257(03)00139-1.